Observation of Nanoscale 180° Stripe Domains in Ferroelectric $PbTiO_3$ Thin Films

S. K. Streiffer,[1,*] J. A. Eastman,[1] D. D. Fong,[1] Carol Thompson,[1,2] A. Munkholm,[3] M. V. Ramana Murty,[1,†] O. Auciello,[1] G. R. Bai,[1] and G. B. Stephenson[1]

[1]*Materials Science Division, Argonne National Laboratory, Argonne, Illinois 60439*
[2]*Physics Department, Northern Illinois University, DeKalb, Illinois 60115*
[3]*Lumileds Lighting, San Jose, California 95131*

(Received 27 March 2002; published 19 July 2002)

We report the observation of periodic 180° stripe domains below the ferroelectric transition in thin films. Epitaxial $PbTiO_3$ films of thickness $d = 1.6$ to 42 nm on $SrTiO_3$ substrates were studied using x-ray scattering. Upon cooling below T_C, satellites appeared around Bragg peaks indicating the presence of 180° stripe domains of period $\Lambda = 3.7$ to 24 nm. The dependence of Λ on d agrees well with theory including epitaxial strain effects, while the suppression of T_C for thinner films is significantly larger than that expected solely from stripe domains.

DOI: 10.1103/PhysRevLett.89.067601 PACS numbers: 77.80.Bh, 61.10.Eq, 64.70.Nd, 68.55.–a

Periodic domain patterns occur in ferroelectric materials because of a fascinating competition between polarization, strain, and electric field [1]. In particular, 180° stripe domains, in which the polarization forms a transverse wave with alternating sign between adjacent lamella, have long been known to occur in bulk ferroelectric single crystals in order to minimize the energy of the electric field arising from the polarization distribution (the ''depolarizing field,'' E_d) [2]. The presence of such stripe domains indicates that E_d has not been eliminated by alternative mechanisms, such as neutralization by surface charge [3]. Recently there has been increased interest in the possibility that 180° stripe domains may often occur in and significantly influence the properties of very thin ferroelectric films [4–7]. Their presence is expected to depend sensitively on the conductivity of the film and the electrical boundary conditions [8–10], such as the existence of extremely thin surface dielectric layers [7]. Calculations including the effects of E_d and domains indicate that the transition temperature T_C can be significantly depressed [4,5], and the dielectric response enhanced [6], relative to the field-free monodomain state. Although such predictions have been invoked to explain the observed depression of T_C in ferroelectric-paraelectric multilayers [11], to date there has been no direct experimental evidence for equilibrium 180° stripe domains in ferroelectric thin films.

In this Letter, we report observations of 180° stripe domains in sub-50-nm-thick epitaxial films of $PbTiO_3$ grown on $SrTiO_3$ (001) substrates, as a function of temperature T and film thickness d. Our approach is to use synchrotron x-ray scattering to observe domain formation and evolution as the sample is cooled from above T_C to room temperature. The experiments were performed at the BESSRC beam line 12-ID-D at the Advanced Photon Source, using an apparatus for *in situ* grazing-incidence x-ray scattering measurements during and following film growth by metal-organic chemical vapor deposition [12]. Typical growth conditions have been described previously [13]. Here we report on films with thicknesses from 1.6 to 42 nm, which were fully epitaxially strained (i.e., in-plane lattice matched to $SrTiO_3$). The films were pure c domain (i.e., polar c axis normal to the film surface) except for $T <$ 500 K in thicker films. This agrees with theory based on the $\sim$1.2% compressive epitaxial strain [14]. An x-ray energy of 24 keV and an incidence angle of 1° were used. *In situ* measurements in the growth chamber not only gave us precise control over film thickness during growth, but also allowed us to provide a vapor pressure of PbO over the film sufficient to maintain stoichiometric $PbTiO_3$ as the equilibrium phase, which is critical for studies of thin films at temperatures above 850 K [13].

Figure 1 shows in-plane x-ray scattering profiles through a $PbTiO_3$ Bragg peak at various temperatures, for a typical film. As T is lowered through T_C, first-order satellite peaks develop around the Bragg peak at positions $\Delta Q = \pm Q_0$, indicating the presence of an in-plane modulation with well-defined period $\Lambda = 2\pi/Q_0$. At about 100 K below T_C, the first-order satellites shift to smaller Q_0, and peaks appear at the higher, odd-order satellite positions $\Delta Q = \pm nQ_0$ ($n = 3, 5, \ldots$). Finally, at about 400 K below T_C, the satellites disappear. At a given temperature the positions and intensities of the satellites do not change with time and are very reproducible provided that T is lowered monotonically from above T_C. For a given T and d, similar satellite patterns with identical spacings Q_0 are observed around all Bragg peaks HKL except those with no out-of-plane component ($L = 0$). The lack of satellites around $L = 0$ peaks implies that the polarization is solely in the out-of-plane direction (positive or negative c domains). The lack of even-order satellites is consistent with the 1:1 ratio of positive and negative domains expected for field cancellation. The T dependences of both the Bragg and satellite intensities are consistent with those expected from increasing polarization below T_C. These characteristics confirm that the satellite scattering originates from 180° stripe domains.

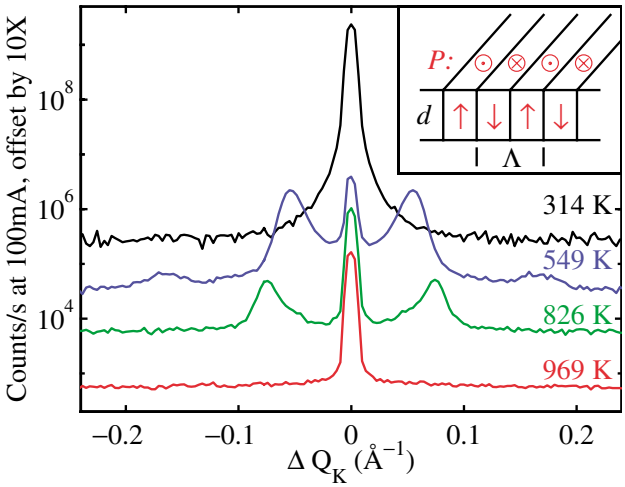

FIG. 1 (color). In-plane x-ray scans through the $PbTiO_3$ 304 peak for a 12.1-nm-thick film, at various temperatures. Inset: Schematic of 180° stripe domains.

Typical in-plane arrangements of the satellite pattern are shown in Fig. 2. On various samples, the satellites either form rings 2(a) and 2(c), are aligned in the H and K directions 2(b), or are aligned at a particular azimuth 2(d). These are all consistent with linear stripe domains, oriented either randomly, crystallographically, or in a single direction, respectively, within the illuminated area (1 mm^2). We confirmed on several samples showing unidirectional alignment that the stripe orientation corresponds to that of the terraces on the surface that occur due to substrate miscut [typical 0.25° vicinal angle from (001)]. Such alignment increases the prominence of the higher-order satellites in phase F_β, as in Fig. 2(d). Both the central Bragg peak and the satellites show thickness fringes in the out-of-plane (L) direction with a spacing $\Delta Q_L = 2\pi/d$, indicating that the stripe structure extends through the film.

Figure 3 shows a typical temperature dependence of the stripe period Λ for a given thickness film. As T is lowered, Λ changes fairly abruptly from a lower to a higher value. We interpret this to be a transition between two stripe domain phases, F_α and F_β. The stripe periods vary systematically with film thickness in both phases, as shown in Fig. 4(a). The lack of higher-order satellites in the F_α phase suggests that the 180° domain walls are significantly more diffuse in F_α than F_β.

We determined T_C for films of various thickness by measuring the T dependence of the out-of-plane lattice parameter c. Typical data are shown in Fig. 3. Owing to its large coupling to polarization, epitaxial strain is expected to significantly affect the ferroelectric transition. Recent calculations [15] for $PbTiO_3$ films, in which the electric field is assumed to be zero, predict that the epitaxial constraint changes the order of the transition from first to second, and that T_C can be elevated significantly above the zero-stress value of $T_C^{zs} = 765$ K. When the effects of electric field and stripe domains are included [2,5], this zero-field result is valid in the limit of a thick film ($d \to \infty$). For fully strained $PbTiO_3$ on $SrTiO_3$, the predicted $c(T)$ in the thick-film limit is shown in Fig. 3 [16]. The transition is located at the abrupt change in slope of $c(T)$ at $T_C^\infty = 1025$ K. We observe just such a slope change with no discrete jump in our $c(T)$ data, confirming that the transition is continuous. The values of T_C obtained from

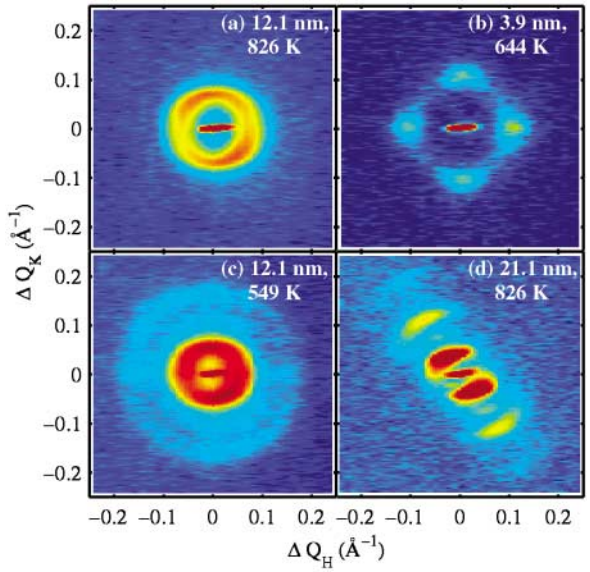

FIG. 2 (color). Typical in-plane distributions of satellite intensity around the $PbTiO_3$ 304 peak, for various d and T. Redder hue indicates higher intensity (log scale). (a) and (b) are phase F_α; (c) and (d) are phase F_β. Elongation of central Bragg peak is due to asymmetric resolution function.

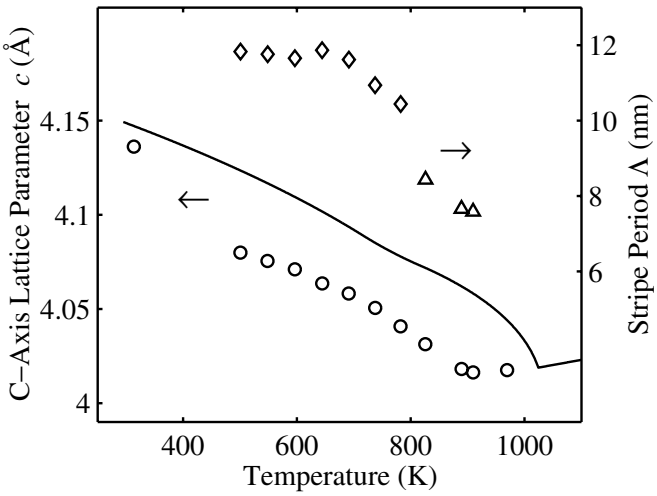

FIG. 3. Stripe period Λ and lattice parameter c as a function of T for a 12.1-nm-thick $PbTiO_3$ film. Symbols for Λ correspond to the phase, F_α (triangle) or F_β (diamond). Symbols for c are circles; line shows calculated c for epitaxial $PbTiO_3/SrTiO_3$ film with $E = 0$ (thick film limit).

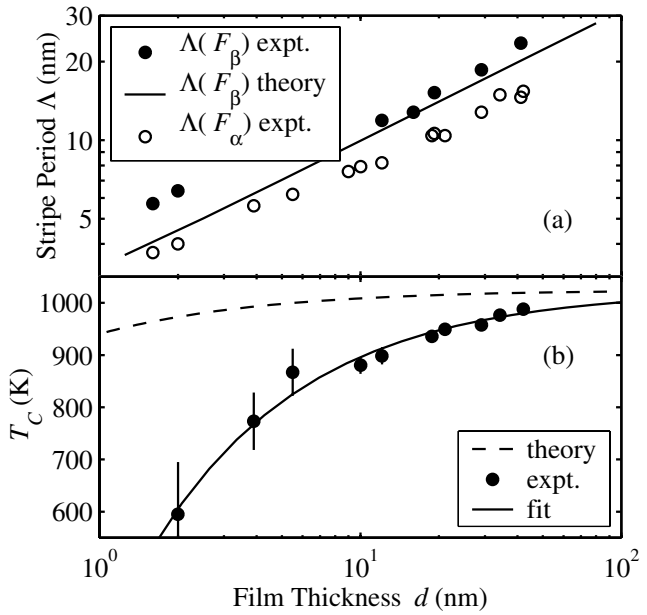

FIG. 4. (a) Stripe period Λ vs thickness d. Solid symbols: phase F_β at $T = T_C - 250$ K. Open symbols: phase F_α at $T = T_C - 50$ K. Line: sharp wall theory at $T = T_C - 250$ K. (b) T_C vs d. Symbols with error bars: observed values. Solid line: fit to $T_C/T_C^\infty = 1 - (d/d_0)^{-n}$, with $d_0 = 0.59$ nm, $n = 0.73$. Dashed line: theory (see text).

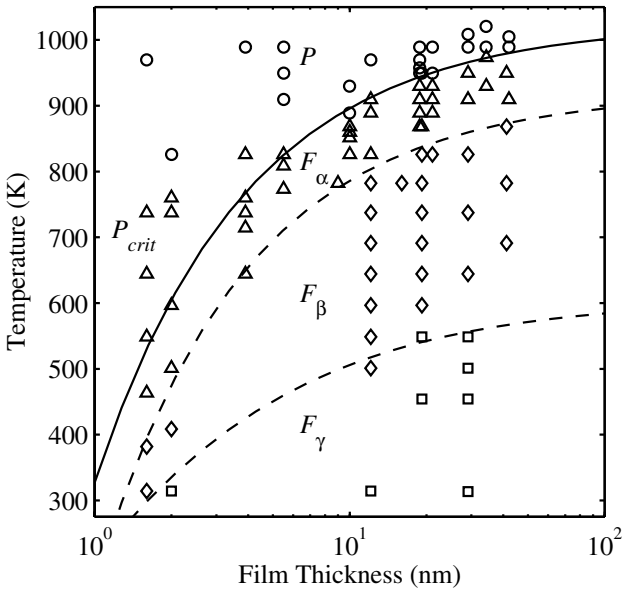

FIG. 5. Phase diagram for epitaxial $PbTiO_3$ thin films on $SrTiO_3$. Solid line: T_C determined from $c(T)$. Circles: no satellites, paraelectric phase P. Triangles: satellites at larger Q_0, ferroelectric stripe phase F_α or critical fluctuations $P_{\rm crit}$. Diamonds: satellites at smaller Q_0, ferroelectric stripe phase F_β. Squares: no satellites, ferroelectric monodomain phase F_γ. Dashed lines: estimated phase boundaries.

the measured $c(T)$ are shown as a function of film thickness in Fig. 4(b). For thicker films we observe that T_C is elevated well above T_C^{zs}, approaching the predicted value of T_C^∞ as $d \to \infty$. However, as d decreases, T_C is suppressed hundreds of K below T_C^∞.

Figure 5 shows the observed phase diagram as a function of d and T. The symbol type indicates the presence or absence of x-ray satellites, and whether the stripe period corresponds to the lower (F_α) or higher (F_β) value. Also shown (solid line) is T_C determined from the lattice parameter. For film thicknesses above 5 nm, the appearance of satellites corresponds closely to T_C. For thinner films, measurable satellites occur above T_C, consistent with stronger critical point fluctuations as the system becomes two dimensional. The phase without satellites at low T we label F_γ. We believe that F_γ is the monodomain ferroelectric phase, since c is close to the zero-field prediction (see Fig. 3), indicating that E_d has been relaxed without 180° stripe domain formation.

We can compare the results in Fig. 4 to theory with no adjustable parameters, since all the required properties of the $PbTiO_3/SrTiO_3$ system have been obtained independently. For stripes with sharp domain walls, corresponding to phase F_β, an analytical solution has been obtained in a linearized model in which P varies linearly with E in each domain. The original treatment for thick films [2] has recently been extended to thin films, in which the regions of nonzero E near the surfaces overlap [5]. We expect that the boundary conditions for our case will be asymmetric: the outer surface of the film will be compensated by free charge, since it is exposed to a reactive atmosphere, while the interface between the $PbTiO_3$ film and the $SrTiO_3$ substrate will be isolated from free charge. The polarization distribution is thus equivalent to that in one half of a $PbTiO_3$ film of thickness $2d$, having symmetric isolated $SrTiO_3$ boundary conditions at both surfaces [4]. Extending the treatment [5] to include an external dielectric, the equilibrium stripe wave number Q_0 is given by the implicit relation

$$Q_0^2 = \frac{4P_0^{*2}}{\pi\epsilon_{ex}\epsilon_0\gamma d}\sum_{n=1,3,5,\ldots}\frac{1}{n^3} \times\left[\frac{1}{1+g\coth(n\phi)} - \frac{gn\phi}{[\sinh(n\phi)+g\cosh(n\phi)]^2}\right], \quad (1)$$

with $\phi \equiv (\epsilon_1^*/\epsilon_3^*)^{1/2} Q_0 d$ and $g \equiv (\epsilon_1^*\epsilon_3^*)^{1/2}/\epsilon_{ex}$, where ϵ_1^* and ϵ_3^* are the dielectric constants of the film perpendicular and parallel to the polarization direction, ϵ_{ex} is that of $SrTiO_3$ [17], P_0^* is the equilibrium polarization under zero field, and γ is the 180° domain wall energy. Here ϵ_1^*, ϵ_3^*, and P_0^* are the renormalized values for the epitaxially strained film [18]. Recent calculations of the 180° domain wall energy at $T = 0$ K give $\gamma(0) = 132$ mJ/m^2 [19]. Since the domain wall energy is expected to be proportional to P_0^{*3} [2], its temperature dependence can be estimated as $\gamma(T) = \gamma(0)[P_0^*(T)/P_0^*(0)]^3$. In the limit $\phi \gg 1$, which in our case applies for $d > 10$ nm,

Eq. (1) reduces to $Q_0 = 1.16P_0^*[\epsilon_0\epsilon_{ex}(1+g)\gamma d]^{-1/2}$, giving Λ proportional to $d^{1/2}$. The dependence of Λ on T is relatively weak [2]. The predicted stripe period as a function of d is shown in Fig. 4(a). The data and model are in strikingly good agreement, considering that there are no adjustable parameters. This provides quantitative support for the calculations of $\gamma(0)$ [19] and the effects of epitaxial strain [15].

The linearized model predicts that the stripe domains become ineffective at neutralizing E_d in sufficiently thin films, so that T_C depends on d. The critical thickness below which the ferroelectric phase is not stable can be obtained as $d_C = 1.53\epsilon_0\epsilon_3^{*2}\gamma/\epsilon_{ex}(1+g)P_0^{*2}$. Inverting $d_C(T)$ gives $T_C(d)$, which is shown in Fig. 4(b). The observed suppression of T_C for thin films is much larger than this prediction. One explanation for this discrepancy is the linearization of $P(E)$ in the model [9]. However, since the linearization overestimates the free energy of the F_β phase, the predicted suppression of T_C will be even smaller in a full nonlinear solution, in disagreement with the data. An alternative explanation is suppression of the polarization at the surface due to intrinsic effects, which have typically been described using additional terms in the mean-field free energy functional [20]. The physical origins and consequences of these effects are a subject of continuing investigation [21].

The observation of three ferroelectric phases can be qualitatively understood using existing concepts. The F_α phase observed just below T_C has a smaller stripe period and more diffuse domain walls than the F_β phase. It has been proposed that polarization-wave fluctuations in the paraelectric phase become unstable at T_C, forming a 180° stripe domain phase with diffuse walls [10,22]. A gradient energy term of the form $\kappa|\nabla \times P|^2$ is used to represent the domain wall energy. Like the sharp wall theory for F_β, this diffuse wall theory for F_α predicts a stripe period proportional to $d^{1/2}$. Depending on the relationship used to obtain κ from γ, the predicted stripe period for F_α is similar to or smaller than that for F_β, as observed. At lower T, nonlinearity in the free energy functional is expected to favor sharp domain walls [22]. The transition to the monodomain ferroelectric phase F_γ has been predicted by treating the ferroelectric as a semiconductor, in which carriers can be created by the field effect. The critical thickness for monodomain formation has been given as [9] $d_C = 2.6\epsilon_0\epsilon_3^*\Phi/P_0^*$, where Φ is the potential difference between the Fermi level and the conduction band. Using $\Phi = 1.9$ V (half the optical band gap of $PbTiO_3$), monodomain formation is predicted to occur at a polarization corresponding to $T_C - T = 325$ K for $d = 10$ nm, in qualitative agreement with our observations. The rich phase diagram we have observed in this simple system makes it an excellent test case for more quantitative development of these concepts.

For the thin films described here, T_C is above room temperature. The fit to $T_C(d)$ predicts that even two-unit-cell- (0.8-nm-) thick films would be ferroelectric at low T. This is in agreement with expectations based on the increase in T_C from epitaxial strain, counteracted by the intrinsic thickness effect [21]. Further study of ultrathin films will be required to determine whether the surface, which forms an antiferrodistortive reconstruction [23], also participates in the ferroelectricity.

We acknowledge capable experimental assistance from L. Thompson, M. E. M. Aanerud, and the BESSRC beam line staff. This work was supported by the U.S. Department of Energy, BES-DMS under Contract No. W-31-109-ENG-38, and the State of Illinois under HECA.

*Electronic address: streiffer@anl.gov
†Current address: E2O Communications Corp., 26679 W. Agoura Road, Calabasas, CA 91302.

[1] J. S. Speck and W. Pompe, J. Appl. Phys. **76**, 466 (1994).
[2] T. Mitsui and J. Furuichi, Phys. Rev. **90**, 193 (1953).
[3] Y. Watanabe, M. Okano, and A. Masuda, Phys. Rev. Lett. **86**, 332 (2001).
[4] Y. G. Wang, W. L. Zhong, and P. L. Zhang, Phys. Rev. B **51**, 5311 (1995).
[5] A. Kopal, T. Bahnik, and J. Fousek, Ferroelectrics **202**, 267 (1997).
[6] A. M. Bratkovsky and A. P. Levanyuk, Phys. Rev. B **63**, 132103 (2001); A. Kopal *et al.*, Ferroelectrics **223**, 127 (1999).
[7] A. M. Bratkovsky and A. P. Levanyuk, Phys. Rev. Lett. **84**, 3177 (2000); **85**, 4614 (2000); **87**, 179703 (2001).
[8] Y. Watanabe and A. Masuda, Jpn. J. Appl. Phys. **40**, 5610 (2001); A. M. Bratkovsky and A. P. Levanyuk, Phys. Rev. B **61**, 15 042 (2000).
[9] E. V. Chenskii, Sov. Phys. Solid State **14**, 1940 (1973).
[10] E. V. Chenskii and V. V. Tarasenko, Sov. Phys. JETP **56**, 618 (1982).
[11] E. D. Specht *et al.*, Phys. Rev. Lett. **80**, 4317 (1998).
[12] G. B. Stephenson *et al.*, MRS Bull. **24** (1), 21 (1999).
[13] M. V. Ramana Murty *et al.*, Appl. Phys. Lett. **80**, 1809 (2002).
[14] N. A. Pertsev and V. G. Koukhar, Phys. Rev. Lett. **84**, 3722 (2000).
[15] N. A. Pertsev, A. G. Zembilgotov, and A. K. Tagantsev, Phys. Rev. Lett. **80**, 1988 (1998).
[16] Lattice parameters of $SrTiO_3$ and cubic $PbTiO_3$ from Y. S. Touloukian *et al.*, *Thermal Expansion-Nonmetallic Solids* (Plenum, New York, 1977), and M. J. Haun *et al.*, J. Appl. Phys. **62**, 3331 (1987), respectively.
[17] F. Jona and G. Shirane, *Ferroelectric Crystals* (Macmillan, New York, 1962).
[18] $\epsilon_i^* = 1 + (2a_i^{*\prime})^{-1}$, $a_1^{*\prime} = a_1^* + a_{13}^* P_0^{*2} + a_{112} P_0^{*4}$, $a_3^{*\prime} = a_3^* + 6a_{33}^* P_0^{*2} + 15a_{111} P_0^{*4}$, and $P_0^{*2} = [-a_{33}^* + (a_{33}^{*2} - 3a_3^* a_{111})^{1/2}]/3a_{111}$, where the a_i are from Ref. [15].
[19] B. Meyer and D. Vanderbilt, Phys. Rev. B **65**, 104111 (2002).
[20] R. Kretschmer and K. Binder, Phys. Rev. B **20**, 1065 (1979).
[21] A. G. Zembilgotov *et al.*, J. Appl. Phys. **91**, 2247 (2002).
[22] P. N. Timonin, JETP **83**, 503 (1996).